Angewandte Chemie
Eine Zeitschrift der Gesellschaft Deutscher Chemiker

Supporting Information

69451 Weinheim, Germany

Real Hierarchical Architecture with Nanostorage on the Nacreous Layer and Its Mimetic

Yuya Oaki and Hiroaki Imai*

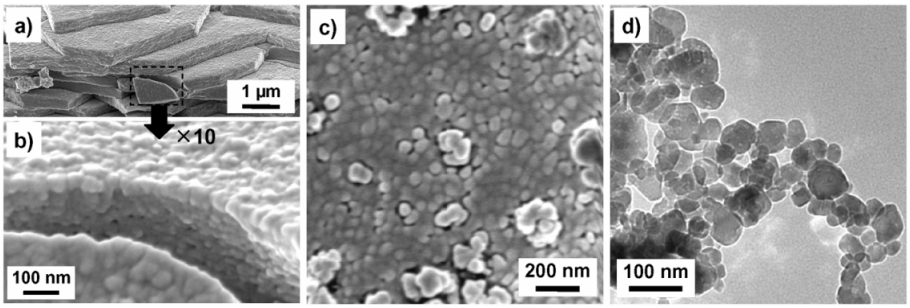

Figure S1. FESEM (a–c) and FETEM (d) images of the inside of an aragonite plate (artificially induced pearl). a) partially fractured plate in the nacreous layer; b) the magnified image of panel a); c) the powdered sample by a mortar; d) the powdered sample observed by FETEM. The images in panels a) and b) clearly show that an aragonite platy unit consisting of the nano-building blocks with a size of several tens nanometers. The same sizes of the nano-building blocks were observed in the powdered samples (panel c). The samples were coated by amorphous osmium thin film to avoid the obstruction of sputtered Au/Pd particles. To gain the further detailed information, we carried out by FETEM observations. The samples for FETEM observations were simply prepared as follows; the powdered sample as shown in panel c) was dispersed in water using an ultrasonic bath, and then the dispersion liquid was dropped on a copper grid supported with collodion membrane. The same sizes of the nano-building blocks were observed by FETEM (panel d). All the electron microscope analysis was carried out by our own operation. The incorporated organic components interrupted the clear observation of nano-building blocks, but the samples were neither damaged nor miniaturized during the radiation of electron beam. The operating conditions of FESEM and FETEM were described in the Experimental Section. These facts strongly supported that the nano-building blocks were neither attributable to the sample preparation process nor the radiation damage on FETEM observation.

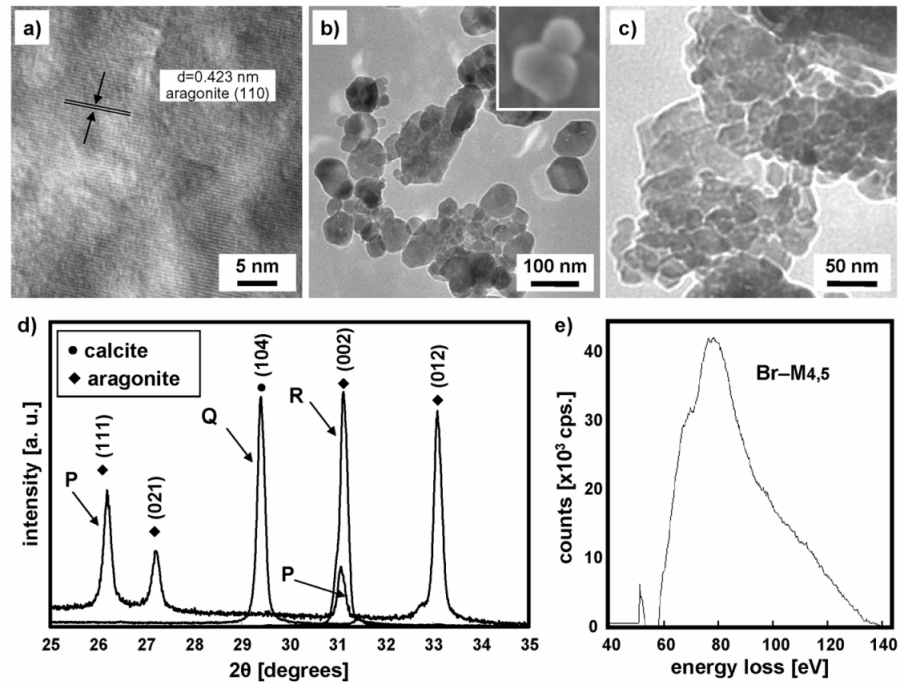

Figure S2. a) The high-resolution TEM image on the fringe of nano-building block. The lattice spacing was 0.423 nm corresponding to the (110) plane of aragonite; b and c) FETEM images of the nano-building blocks in artificially induced pearl and pearly oyster, respectively. The size of the nano-building blocks in pearly oyster (ca. 10 nm) was smaller than that in its artificially induced pearl (ca. 80–150 nm). The further investigations were needed for the size. d) XRD profiles of comminuted powder sample of nacreous layer (P), the nacreous layers horizontally attached to the sample holder (Q), and the calcite powder as a reference (R). The peak broadening was not observed in comminuted powder sample (profile P) by comparison of profiles Q and R. Therefore, we concluded that the nano-building blocks generated oriented assembly. e) EELS chart of bromine from EY molecules included in aragonite/biopolymer composite (background subtracted). The peak was obtained around the area of Figure 1j,k. The EF-TEM mapping as shown in Figure 1k was carried out by three-window method based on this peak (filtering at 75 eV, pre-edge 14 eV, post-edge 10 eV, slit width 10 eV).

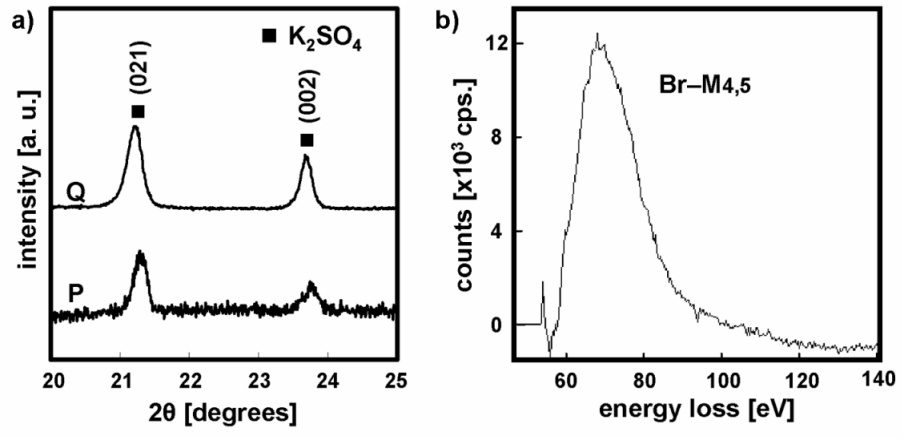

Figure S3. a) XRD profiles of the reference sample (P) and the K_2SO_4/PAA composite. Since the peak broadening was not observed, a unit consisted of the nano-building blocks mediating oriented assembly. b) EELS chart of bromine from EY molecules included in K_2SO_4/PAA composite (background subtracted). The mapping as shown in Figure 2j,k was carried out by the same method and condition as described in Figure S1e.

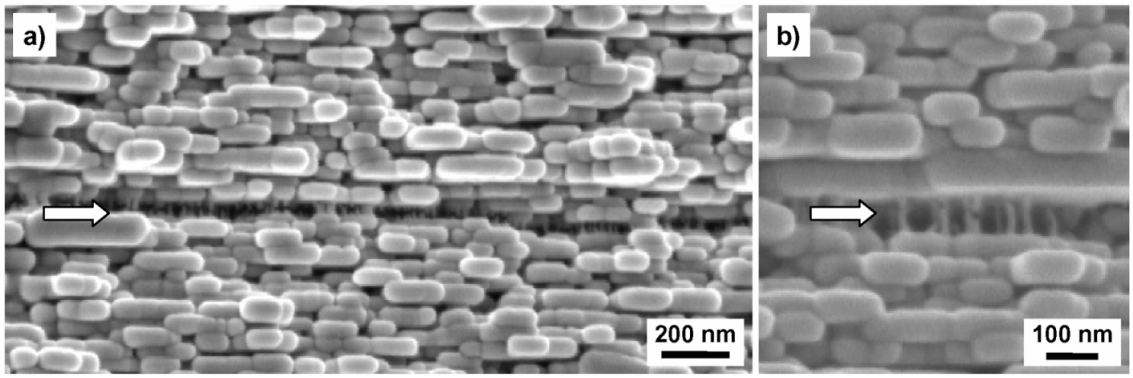

Figure S4. The magnified FESEM images of mineral bridges in K_2SO_4/PAA composite (white arrows). These images clearly indicate the presence of mineral bridges leading to the next layer.

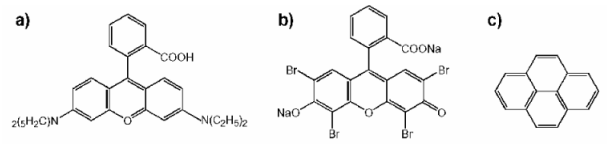

Chart S1. Structural formula of dye molecules as used in this paper. a) rhodamine B (RB, Kanto Chemical, 98.0 %); b) eosin Y (EY, Aldrich Chemical, 89.0%); c) pyrene (PY, Kanto Chemical). These reagents were used without further purification.